DIFFUSE SCATTERING OF RADAR ON THE SURFACE OF VENUS: ORIGIN AND IMPLICATIONS FOR THE DISTRIBUTION OF SOILS

D. L. BINDSCHADLER and J. W. HEAD

Department of Geological Sciences, Brown University, Providence, RI, U.S.A.

(Received 9 March, 1988)

Abstract. Previous analysis of PV altimeter data has shown that ~25% of the surface of Venus is characterized by low values of reflectivity, interpreted as being due to the presence of porous materials such as soils. However, examination of a corrected reflectivity data set in combination with PV altimeter data suggests that no more than 5% of the surface of Venus is covered by soils more than several to tens of cm in depth. Most regions of apparent low reflectivity are instead interpreted to be due to the presence of small (5–50 cm) roughness elements on the surface that cause diffuse scattering at the 17 cm PV wavelength. Regions of low apparent reflectivity are of interest because of a correlation with tessera, a complex tectonic unit mapped from Venera 15/16 SAR data. Regions of tessera are characterized by a complex system of intersecting ridges and valleys thought to be of tectonic origin. Examination of possible models for the form of diffuse scatterers in the tessera suggests that they are rock fragments and originate from a mass-wasting process that is linked to the rugged nature of the terrain. Further, these diffuse scatterers are associated with other tectonic landforms, suggesting that they originate as part of tectonic deformation of the surface. Viewed from a geologic standpoint, the PV data sets are important tools for understanding tectonic, volcanic, and degradational processes on Venus, as well as for future interpretation of data from the Magellan mission.

Introduction

Radar altimetry, reflectivity, and rms slope data obtained by the Pioneer Venus mission (Masursky *et al.*, 1980; Pettengill *et al.*, 1980a, 1982) provide a measure of the topography and surface properties of Venus at approximately 100 km horizontal resolution. The PV synthetic aperture radar (SAR) experiment provides approximately 30 km resolution data for latitudes between 45° N and 15° S. Both of these data sets are of renewed interest given the SAR data obtained by Venera 15 and 16 for the northern quarter of Venus at horizontal resolution of approximately 1–3 km (Kotelnikov *et al.*, 1984; Barsukov *et al.*, 1986). The synoptic view offered by the PV data may aid our understanding of the origin and evolution of the terrains mapped from Venera data (Barsukov *et al.*, 1986).

In this paper we first review the interpretation of the PV radar data of Head *et al.* (1985). Examination of a corrected reflectivity data set (Ford and Pettengill, 1984) suggests that low reflectivity regions in the original PV data should be interpreted as being due to approximately PV wavelength-scale (17 cm) roughness. Previously, low reflectivity regions were thought to reflect the presence of a significant component of porous materials such as soil (Head *et al.*, 1985; Garvin *et al.*, 1985). We also note a high degree of correspondence between low values of reflectivity and a morphologic unit mapped from Venera 15/16 data (Barsukov *et al.*, 1986; Basilevsky *et al.*, 1986) and called tessera. Tessera is characterized by a complex system of intersecting ridges

Earth, Moon, and Planets **42** (1988) 133–149.

and valleys and is interpreted to be tectonic in origin (Basilevsky *et al.*, 1986; Basilevsky, 1986). This correlation of km-scale morphology and surface radar properties led us to examine geological models for the cause of the low values of reflectivity. The model most consistent with available data suggests that the origin of diffuse scatterers is closely linked to fracture of the surface and/or creation of km scale slopes during tectonic deformation. Further support for such a model is an observed association of diffuse scattering with features such as chasmata, which are thought to be tectonically deformed. In a related paper (Bindschadler and Head, 1988a), we discuss more general correlations of the 1–3 km surface morphology (from Venera 15/16 data) with surface reflectivity and roughness properties (from PV data).

PV data

The Pioneer Venus radar mapper obtained near-normal incidence radar measurements of 93% of the surface of Venus at 17 cm wavelength (Pettengill *et al.*, 1980a, b; Masursky *et al.*, 1980). The measured quantities of absolute time delay, time dispersion, and reflected power were used to derive altimetry, roughness, and reflectivity parameters based on the empirical Hagfors law (Hagfors, 1964, 1967, 1970). The surface resolution of the radar data vary from a 23 × 7 km footprint obtained at the periapsis altitute (150 km) to a footprint over 100 × 100 km for data obtained at the 4700 km altitude limit of the mapping instrument (Pettengill *et al.*, 1980a, b).

To interpret the data sets derived from the PV altimeter, Head *et al.* (1985) used an image processing technique of map intersections to examine correlations between altimetry, reflectivity, and roughness data. These workers defined four subdivisions in topography and three each in roughness and reflectivity (Table I). The spatial and statistical distribution of roughness and reflectivity, as well as models relating reflectivity to surface material density (Garvin *et al.*, 1985; Head *et al.*, 1985), were used as a basis for subdividing the surface in terms of these parameters.

ALTIMETRY

A single altimetric measurement is made from an orbiting spacecraft by recording the time delay between the transmission and reception of a nadir-directed radar pulse. With precise knowledge of the spacecraft's orbital position, the radius from the planetary center of mass to a radar 'footprint' on the surface can be calculated (Pettengill *et al.*, 1980a). The spherical shape of a planet and the small-scale roughness of the surface act to disperse the returned signal in time. This effect is illustrated in Figure 1, which is a schematic plot of the echo intensity as a function of time delay for a single transmitted pulse. The elevation measured from this signal is taken from t_0, the time at which the measured intensity reaches a maximum. This elevation will lie well within the actual range of elevations for that footprint, except under very unusual circumstances. For example, large expanses of terrain that lie outside the radar footprint and slope toward the altimeter or are highly radar reflective may cause erroneous readings, but the large areas, high reflectivities, and steep slopes

TABLE 1

Pioneer Venus Units

Surface type[a]	Definition	Area[b]
Elevation[c] (h)		
Lowlands	$h < 0.0$	25%
Rolling plains	$0.0 < h < 2.0$	63%
Highlands	$2.0 < h < 4.5$	10%
Mountainous Regions	$h > 4.5$	2%
RMS Slope (θ)		
Smooth	$1.0° < \theta < 2.5°$	52%
Transitional	$2.5° < \theta < 5.0°$	43%
Rough	$5.0° < \theta < 10.0°$	5%
Reflectivity (ρ)		
Soil/porous material	$\rho < 0.10$	26%
Rock-dominated	$0.10 < \rho < 0.20$	68%
High dielectric	$\rho > 0.20$	6%

[a] Surface types are according to Head *et al.* (1985)
[b] Total area of Venera 15/16 map is 92.2×10^6 km^2.
[c] Elevations are in km relative to radius of 6051.0 km.

(Sharpton and Head, 1985) required for such errors to occur are clearly exceptional and unlikely. An altimetry measurement then indicates that a significant portion of the surface lies at or near the elevation measured.

RMS SLOPE

The time dispersion ('shape') of the radar echo is used to determine the rms slope θ of the surface. This quantity is an indication of the angular distribution of quasi-specular scattering facets on the surface and is related to the observed radar cross-section of the surface via the Hagfors law (Hagfors, 1970)

$$\sigma_0 = (\rho C/2)(\cos^4 \phi + C \sin^2 \phi)^{-3/2}, \tag{1}$$

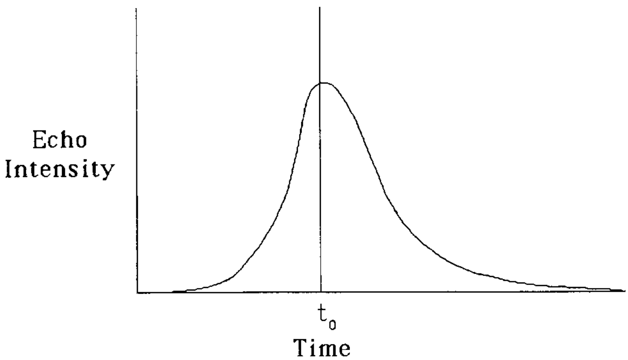

Fig. 1. Schematic plot of the time dispersion of an altimeter echo. The shape and width of the curve is a function of both the spherical geometry of the planet and the rms slope of the surface.

where

σ_0 = specific radar cross section;
ρ = Fresnel reflectivity of the surface;
C = Hagfors C factor;
ϕ = incidence angle of radar signal

the C factor is related to rms slope θ by

$$\theta = 180/(\pi C^{1/2}). \tag{2}$$

In analysis of the PV data, the scattering law given in (1) was used to weight the scattering from surface areas at increasing incidence angle away from the sub-radar point. For the PV altimeter, the maximum incidence angle varied from approximately 5° to 8°, depending on spacecraft altitude (Pettengill *et al.*, 1980a). The weighting process leads to a model for the planetary scattering function, which may then be convolved with known properties of the radar waveform to obtain a prediction of the echo intensity as a function of time (e.g. Figure 1) for a particular set of values of ρ and θ (Pettengill *et al.*, 1980a).

The effect of varying surface roughness on the reflected signal is illustrated by Figure 2. A small but representative portion of the surface of a footprint is shown in Figure 2a. Because the surface here is relatively smooth at the several to tens-of-wavelengths scale, the amount of radar energy scattered back to the altimeter is largely controlled by the spherical figure of the planet. This results in the restriction of most of the reflected signal to a narrow interval in time delay (Figure 2b). The portions of a footprint farthest from the subradar point contribute only a tiny fraction to the total received echo. In Figure 2c, the representative surface is much rougher. Portions of a footprint near the subradar point contribute less to the received echo than in the first case, because more energy is scattered at large angles. Points far from the subradar point contribute more than they did in the case of the smooth surface for the same reason. The result is that the echo is more dispersed in time (Figure 2d) than for a smoother surface.

Implicit in this treatment is the assumption that the roughness elements on the surface have scale lengths on the order of tens to hundreds of wavelengths, or approximately 0.5–10 m for the PV radar system. Roughness elements near the PV wavelength (17 cm), predominantly in the 5–50 cm size range, may cause diffuse scattering of radar energy. This effect is important in some cases and is discussed further in a later section. Roughness elements much larger than 10 m (e.g. km-scale topography) may also contribute to rms slope measurements. However, radar measurements of roughness on Mars and comparison with Viking orbiter images suggests that the scale of roughness responsible for radar scattering is too small to be reliably inferred from topography at scales of 100's to 1000's of meters (Simpson *et al.*, 1984).

The rms slope data thus yield a comparative measure of surface roughness at a scale of 0.5–10 m, but do not uniquely characterize the shape of the surface at these scales. The undulatory surface in Figure 2c can be characterized by the same values

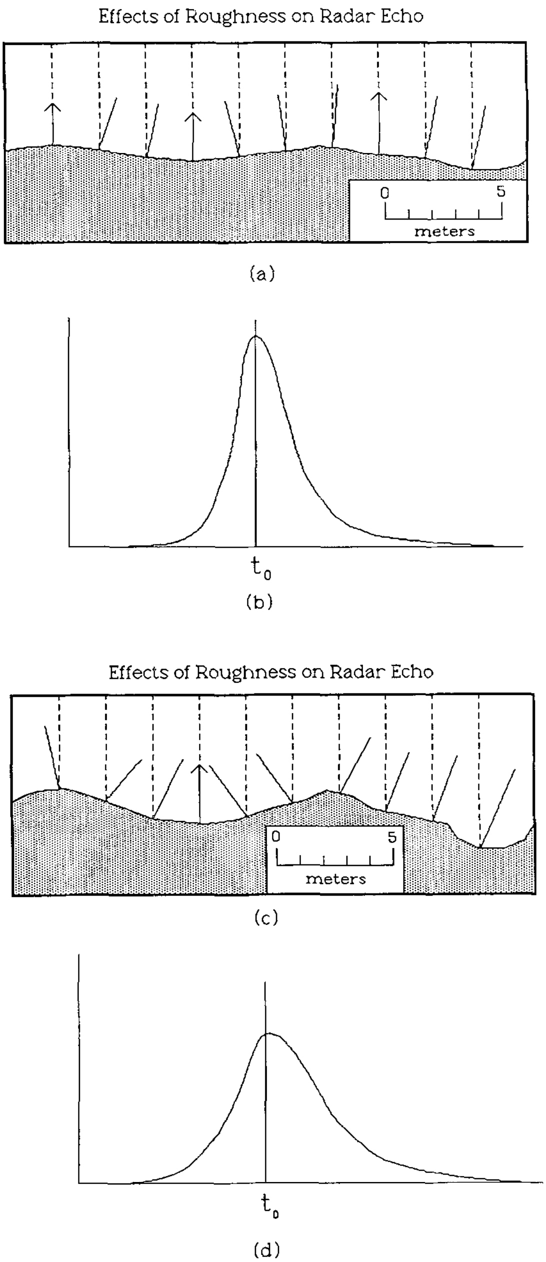

Fig. 2. Effects of roughness at 10-100 wavelength scales on altimeter echoes. (a) Relatively low rms slope in this area means that much of the incident radiation (dotted lines) is reflected (solid lines) to the altimeter. (b) Time-delay shape of an echo typical of the surface in 2a. (c) Relatively rough surface (at 10–100 wavelength scales). Note that the altimeter will make no distinctions between the continuously undulating surface to the left and the more discontinuously sloping surface on the right. (d) The broader time-dispersion shape is characteristic of the high rms slope value of the surface in figure 2c. The area under curves 2b and 2d is almost identical, indicating that the rms slope should not affect reflectivity measurements.

of rms slope found for a partially block-covered surface or a tilted, fractured surface. On the basis of comparisons with rms slope values for the Moon and Mars, Head *et al.* (1985) suggested three divisions in rms slope (Table I): (1) smooth surfaces, $\theta < 2.5°$, typical of the smoothest surfaces on Mars; (2) transitional surfaces, $2.5° < \theta < 5.0°$, typical of the lunar maria; (3) rough surfaces, $\theta > 5.0°$, with rms slopes typical of the lunar highlands and roughest portions of Mars.

REFLECTIVITY

The reflectivity ρ is the Fresnel reflection coefficient of a smooth surface at normal incidence (Pettengill *et al.*, 1982) and is extracted from radar data via the Hagfors law (1). The radar reflectivity of a given footprint is determined from the area under curves such as those shown in Figures 2b and 2d. The greater the reflectivity of a surface, the higher the intensity of an echo at a given time, and thus the greater the integrated intensity (or power) of the echo.

Examples of the variations in surface material properties that strongly affect measured reflectivity are shown in Figure 3. In each of the cases A–D, the dashed line denotes the incident radar pulse and the thick arrow denotes the intensity of the echo returned to the altimeter. In the case of A, the radar pulse encounter a surface dominated by some highly porous material such as an unwelded tuff, poorly lithified sediments, or soil. The relatively low intensity of the returned signal is a function of the porosity of this material. In case B, the high intensity of the radar echo indicates a surface that is enriched in some material with a high dielectric constant, such as an extremely Ti-rich basalt or a rock varnish highly enriched in metallic oxides. In case C, the surface consists of either bedrock or blocks composed of silicates with typical

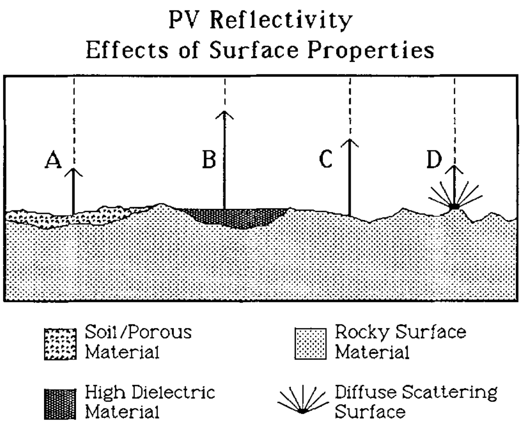

Fig. 3 The effects of surface material properties on radar reflectivity. Dashed lines denote the direction of incoming radiation, while the thick solid lines indicated reflection. Length of the latter is proportional to the power reflectivity ρ. Soil/porous materials (A) and diffusely scattering areas (D) yield the same value of ρ despite their marked differences in porosity. In B and C, the reflectivity of the surface is most strongly influenced by the composition (abundant high dielectric phases vs. typical dielectric silicates) of surface materials.

dielectric properties and yields an intermediate value of reflectivity. In case D, the presence of abundant near-wavelength facets causes diffuse scattering of much of the incident radar pulse. Although the surface is actually dominated by normal rocky materials, the altimeter 'sees' a value of reflectivity characteristic of a much more porous surface. This occurs because diffuse scattering randomizes the angle through which radar is scattered, reflecting much of the incident radiation away from the altimeter.

As long as diffuse scattering is a relatively minor effect, reflectivity data can be treated as a measure of the bulk dielectric constant of the rocks and soil on the surfaces and can be directly related to the density of surface materials (Garvin *et al.*, 1985). Empirical relations for dielectric constant as a function of density have been found from experiments by Krotikov and Troitsky (1963) and Olhoeft and Strangway (1975). In order to derive a relation between the density γ and reflectivity ρ of a surface, these empirical results were combined (Garvin *et al.*, 1985). The obtained relation is given as

$$\gamma = 3.2 \ln\{(1 + \rho^{1/2})/(1 - \rho^{1/2})\}. \tag{3}$$

We note (1) that $\gamma < 2.0$ g cm^{-3} strongly suggests a surface dominated by porous materials such as soils, weakly lithified sediments, highly vesiculated rocks, or unwelded tuffs, and (2) that values of reflectivity at similar wavelengths on the Moon and Mars are almost uniformly < 0.10 (Tyler and Howard, 1973; Tyler *et al.*, 1976). Garvin *et al.* (1985) defined three subdivisions in reflectivity: (1) $\rho < 0.1$ and $\gamma < 2.0$ g cm^{-3}, corresponding to surfaces dominated by highly porous materials; (2) $0.1 < \rho < 0.2$ and $2.1 < \gamma < 3.1$, indicating a surface dominated by low porosity materials such as typical igneous, sedimentary, or metamorphic rocks, (3) $\rho > 0.2$ and $\gamma > 3.1$, corresponding to surfaces enriched in some high dielectric phase (e.g. Fe or Ti oxides).

Corrected reflectivity

This interpretation of reflectivity data is dependent on the assumption that diffuse scattering of radar energy is a relatively minor effect on the surface of Venus. This assumption has been tested by using the PV SAR experiment data to estimate the diffuse scattering behavior of the surface (Ford and Pettengill, 1984). Side-looking radar image data were obtained by the PV orbiter below an altitude of 550 km, effectively restricting coverage to an equatorial belt between 15° S and 45° N latitude (Pettengill *et al.*, 1980a). Unlike the nadir-pointing orientation used to obtain altimetry, SAR data were obtained at angles of incidence between 30° and 58° (Pettengill *et al.*, 1980a). At these angles of incidence, a pure Hagfors law surface will scatter very little radar energy back at the instrument. Most of the reflected signal can then be assumed to be due to diffuse scattering. Given two regions with equal bulk dielectric properties (e.g. areas C and D in Figure 3), the region with the greater abundance of diffuse scatterers (D) will backscatter more of an incident side-looking radar signal to the receiving antenna than will the region with only sparse diffuse scatterers (C).

To correct the PV reflectivity data for potential effects due to diffuse scattering, a phenomenological model for the diffuse scattering behavior of the surface was derived using the SAR image data (Ford and Pettengill, 1984). All SAR measurements within 1/2° of a given PV reflectivity measurement were averaged and entered into the diffuse scattering model to determine the percentage of reflected radiation that was scattered diffusely (P. Ford, pers. comm.). Assuming that the diffuse and specular components of the signal summed to one, Ford and Pettengill (1984) applied correction factors to the reflectivity data within the region where SAR data was of sufficient quality (20° S to 50° N). This correction has a net effect of raising the mean reflectivity for the whole region only a few percent. However, our comparison of the corrected reflectivity with the 1985 NSSDC Pioneer Venus uncorrected reflectivity data shows that the upward revision in ρ for areas within the equatorial region is significant (upward revision of ρ by $> 50\%$).

Analysis

In order to understand the relationships of the reflectivity correction to the rms slope parameter and to the uncorrected reflectivity values, the reflectivity correction factor α (Ford and Pettengill, 1984) was examined for all six divisions in reflectivity and roughness noted previously and for all of the nine possible combinations of these divisions shown in Table I. This correction factor represents the percentage of diffusely scattering material on the surface; values range from 0.0 to ~0.8. It is given by

$$\rho_0 = (1 - \alpha)\rho_c, \tag{4}$$

where ρ_0 is the uncorrected reflectivity and ρ_c is the corrected value of reflectivity. Figure 4 is a map of α for the equatorial region of Venus (20° S to 50° N). It was produced from the 1985 NSSDC Pioneer Venus data using the same techniques employed by the USGS in producing the Pioneer Venus maps of topography and rms slope (USGS, 1981).

In general, plains regions appears relatively dark to moderate in Figure 4 and are characterized by values of $\alpha \leqslant 0.25$. A large swath of plains from ~330° E to 180° E is dominated by very low values of α (<0.15) indicating a very smooth surface at the 5–50 cm scale. RMS slope data show that this area is also relatively smooth at the 0.5–10 m scale (Head *et al.*, 1985). In contrast, plains lying between Atla Regio and Beta Regio (210° E to 270° E) are characterized by highly variable values of α. Areas that appear smooth in PV topography also tend to be relatively dark in Figure 4. Values of α up to 0.5 are found within linked topographic depressions between Ulfrun and Asteria Regiones (225° E to 270° E). Upland regions such as Aphrodite Terra, Phoebe Regio, and Tellus Regio appear very bright and are characterized by values of $\alpha > 0.25$ and common occurrence of $\alpha > 0.50$. The highest values of α are found within central Phoebe Regio, western Tellus Regio, Devana Chasma to the south of Theia Mons, and within or near chasmata in Aphrodite Terra. Tellus Regio and Devana Chasma are known to be tectonically deformed (Basilevsky *et al.*, 1986; Sukhanov, 1986; Bindschadler and Head, 1987; Campbell *et al.*, 1984), while Aphrodite Terra is thought to be tectonically 'disrupted' (Schaber, 1982) and may be a locus of extensional deformation (Head and Crumpler, 1987).

Means and standard deviations for the fifteen distributions of α in rms slope, reflectivity, and their combinations are shown in Table II. The three divisions in rms slope (0.5–10 m roughness) show increasing percent diffuse scatterers with increasing rms slope. Smooth surfaces are the least rough at the 5–50 cm scale, while transitional surfaces are also intermediate in roughness at this scale. Rough surfaces ($\theta > 5.0°$) are very rough at small scales, with a mean α of 40%.

In contrast to the positive correlation of rms slope and diffuse scattering roughness, the three divisions in the uncorrected reflectivity display markedly different correlation with α. Note that we refer to ranges in ρ in terms of the three divisions in reflectivity outlined above and for the uncorrected data. Thus, the term 'rocky surface' refers to a surface with $0.1 < \rho < 0.2$ in the *uncorrected* data set. 'Soil/porous rock' dominated surfaces ($\rho < 0.1$) cover approximately 25% of the surface between 15° S and 45° N, as is the case for the entire PV data set (Head *et al.*, 1985). In the corrected data, these low values of reflectivity are seen over only 5% of the surface. This 80% reduction in area covered by low reflectivity surfaces reflects the large mean value of α (34%) found for such regions (Table II). Rocky surfaces ($0.1 < \rho < 0.2$) are much smoother on average at the diffuse scattering scale; here the mean value of α is comparable to that found for smooth surfaces (i.e. $\theta < 2.5°$). This implies little change in these areas between the corrected and uncorrected reflectivity and thus the interpretation of such areas as rock-dominated is generally not affected. High dielectric surfaces display complex behavior. Unlike the other divisions in reflectivity and rms slope, the percent of diffuse scattering surfaces (α) has an extremely non-Gaussian distribution. Although the mean indicates a relatively large degree of 5–50 cm scale roughness (mean $\alpha = 29.5$), there is a significant group of relatively small values.

The same effects appear in looking at the nine combined reflectivity-rms slope divisions. Rough and 'soil/porous rock dominated' surfaces are characterized by values of α on the order of 30% or greater and are most likely to be areas where significant diffuse scattering occurs. Transitional and smooth surfaces display smaller values of α, on the order of 20% or less (Table II). Rough rocky surfaces are rough at the 5–50 cm scale, but transitional and smooth rocky surfaces are relatively smooth at this scale. High dielectric surfaces display erratic behavior under the reflectivity correction (see Table II).

This analysis and examination of the change between the corrected and uncorrected reflectivity indicate that some of the assignments and interpretations of Head *et al.* (1985) and Garvin *et al.* (1985) require revision. It does not appear to be necessary to reinterpret regions characterized by uncorrected reflectivity values

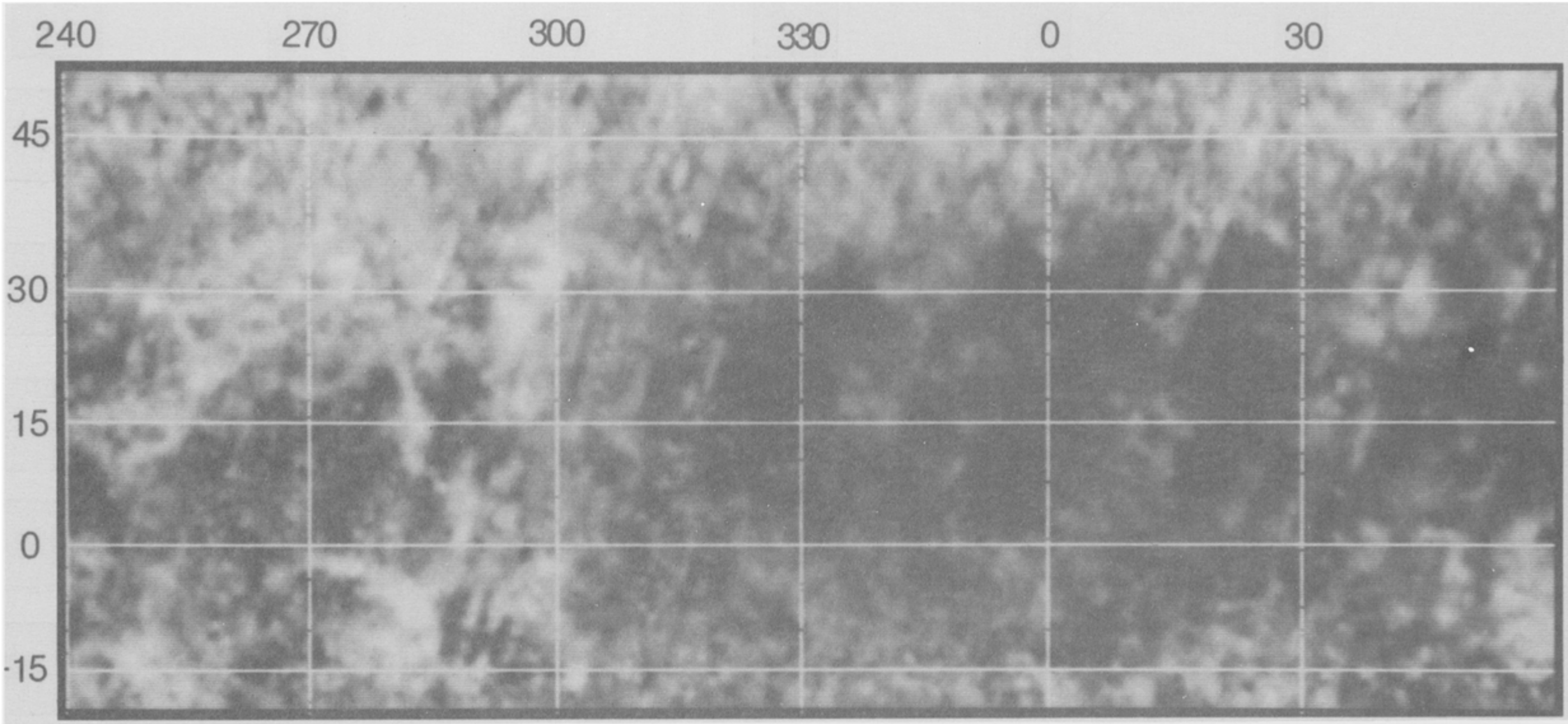

(a) Region from 240° E to 60° E.

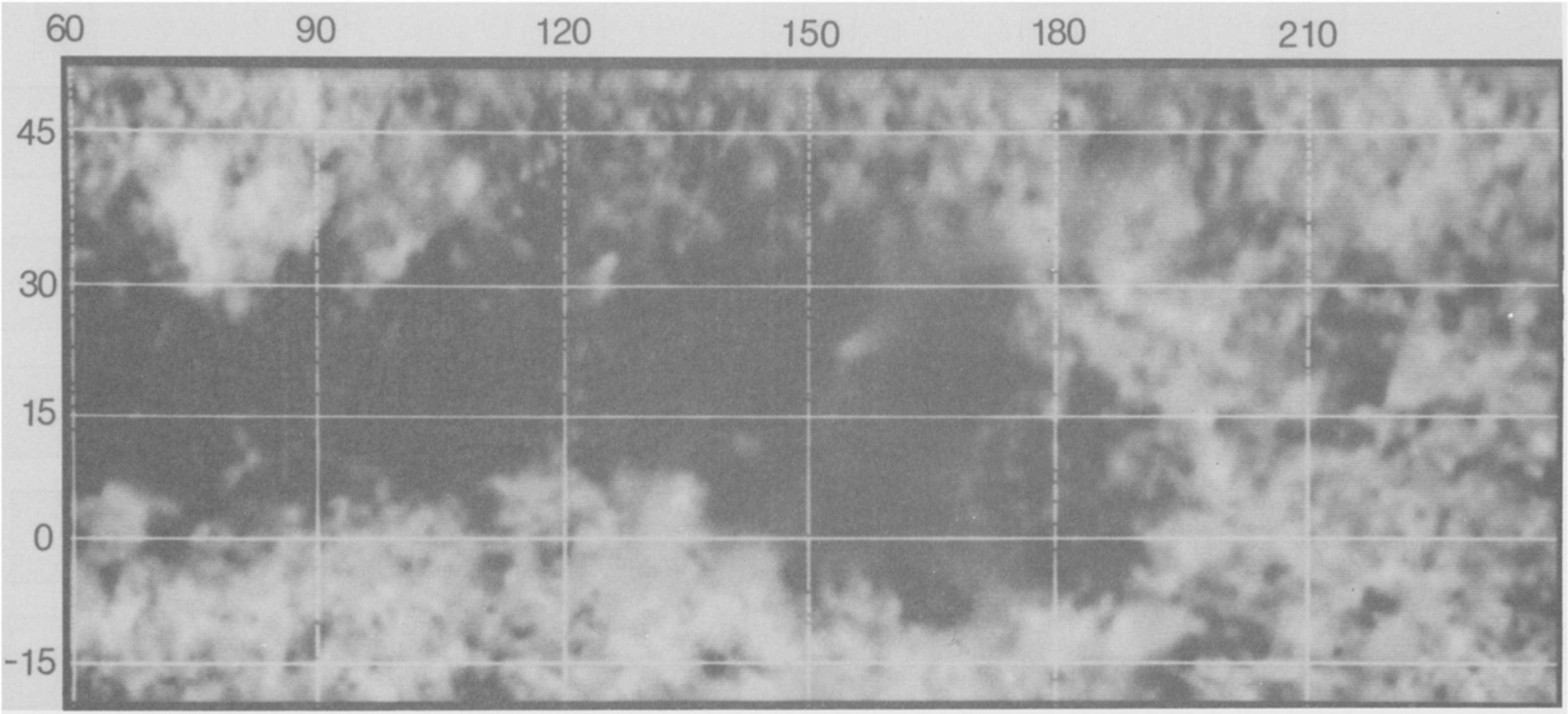

(b) Region from 60° E to 240° E.

Fig. 4. Map showing the percent cover of diffuse scatterers (α) on the surface of Venus as calculated from a correction of PV reflectivity data (Ford and Pettengill, 1984). Latitudes are in degrees east of the prime meridian, longitudes in +degrees north of the equator and −degrees south. The dark band from 315° E to 180° E and ~0° N to 30° N consists of plains characterized by very low values of α. Plains in and around Beta and Aphrodite, as well as higher-altitude plains tend to be characterized by intermediate values of α. The highest values are found within areas such as Tellus Regio, Aphrodite Terra, Phoebe Regio, and Devana Chasma.

TABLE II

Diffuse Scattering Parameter
(for equatorial region)

Surface type[a]	Mean α^b	σ^c
Smooth	0.16	0.11
Transitional	0.24	0.13
Rough	0.40	0.12
Soil/porous material	0.34	0.13
Rock-dominated	0.17	0.11
High dielectric	0.30	0.13
Smooth soils (A)	0.28	0.11
Transitional soils (B)	0.40	0.12
Rough soils (C)	0.47	0.11
Smooth rock (D)	0.14	0.10
Transitional rock (E)	0.19	0.11
Rough rock (F)	0.37	0.11
Smooth h.d. (G)	0.10	0.07
Transitional h.d. (H)	0.23	0.13
Rough h.d. (I)	0.36	0.09

[a] Surface types are from Table I. Letters A–I denote PV surface units of Head *et al.* (1985). "h.d." = high dielectric.
[b] α is the fractional surface area covered by diffuse scatterers for a given region. See equation (4) in text.
[c] σ is the standard deviation of the distribution of α.

ranging from 0.1 to 0.2. Although a few areas (especially rough areas) are revised upward to the high dielectric range of values ($\rho > 0.2$), the effect of the correction leaves the majority of rocky surfaces with values of ρ in the rock dominated range. Regions characterized by high values of reflectivity ($\rho > 0.2$) in the uncorrected data set display behavior under the correction that is not simply interpreted. However, since the revisions are all upward, surfaces with uncorrected $\rho > 0.2$ will continue to be characterized as being dominated by high dielectric materials.

Re-interpretation is required for those regions characterized by low values of uncorrected reflectivity, and originally thought to be dominated by soils and/or porous rock. This is suggested by the large values of α seen in such regions and the consequent extreme decrease in the area covered by regions with $\rho < 0.1$ after the correction. For the equatorial region (20° S to 50° N latitude), approximately 80% of the surface originally characterized as soil-dominated and thought to consist of material with a low dielectric constant is actually better described as normal-dielectric material ($0.1 < \rho < 0.2$) that is rough at a small scale (5–50 cm) and capable of diffusely scattering a significant percentage of incident radar. This revised interpretation of the PV data is shown in Table III.

The pervasive nature of the reflectivity correction within the equatorial region suggests that it is appropriate to extend such a reinterpretation to higher latitudes.

TABLE III

Revised Pioneer Venus Units

Surface type	Definition	Area[a]
Elevation[b] (h)		
Lowlands	$h < 0.0$	25%
Rolling plains	$0.0 < h < 2.0$	63%
Highlands	$2.0 < h < 4.5$	10%
Mountainous Regions	$h > 4.5$	2%
RMS Slope (θ)		
Smooth	$1.0° < \theta < 2.5°$	52%
Transitional	$2.5° < \theta < 5.0°$	43%
Rough	$5.0° < \theta < 10.0°$	5%
Reflectivity (ρ)		
Diffuse scatterers[c]	$\rho < 0.10$	26%
Rock-dominated	$0.10 < \rho < 0.20$	68%
High dielectric	$\rho > 0.20$	6%

[a] Total area of Venera 15/16 map is 92.2×10^6 km^2.
[b] Elevations are in km relative to radius of 6051.0 km.
[c] As much as 5% of surfaces interpreted as diffusely scattering may be soil dominated. See text for explanation.

Although large regions dominated by soil or porous rock cannot be ruled out absolutely, available data suggests that the vast majority of apparently low reflectivity regions are best characterized as diffusely scattering (that is, rough at a 5–50 cm scale) and not as soil-dominated. In addition, correspondence of known or postulated regions of tectonic deformation with high values of diffuse scattering is suggestive of a genetic link.

Discussion

Comparison of Figure 4 to morphologic units mapped from Venera 15/16 SAR data (Barsukov *et al.*, 1986) in the region of overlap of the two shows a correlation of regions of diffuse scattering to a Venera unit called tessera. The highest values of α (Figure 4) are found in Tellus Regio ($\sim$40° N, 80° E), a large region of tessera. Smaller regions of tessera to the east are typically characterized by relatively high values of diffuse scattering. Moreover, regions of tessera north of SAR coverage are characterized by low values of uncorrected reflectivity (Bindschadler, 1986; Bindschadler and Head 1988a). The tessera is tectonic in origin and is characterized by a very complex morphology that may indicate extreme deformation (Basilevsky *et al.*, 1986). Regions of tessera typically rise 1 to 2 km above surrounding plains units and can be identified as such by the presence of numerous linear to curvilinear structures that constitute two distinct intersecting trends (Bindschadler and Head, 1988b). It is the most areally extensive of the tectonic units mapped from Venera data (Bindschadler, 1986; Bindschadler and Head, 1988a) covering $\sim$10% of the region mapped by the Venera orbiters, and is strongly concentrated between a proposed region of crustal convergence in western Ishtar Terra (Crumpler *et al.*, 1986) and a proposed region of crustal divergence in Aphrodite Terra (Head and Crumpler, 1987).

The low values of uncorrected reflectivity observed in the tessera may be interpreted in the context of Venera orbiter and lander data. Four models for the small scale morphology of the surface potentially explain the apparent low reflectivity of the tessera:

(1) The presence of porous materials such as soils, loosely indurated sediments, unwelded tuffs, or highly vesiculated rocks.

(2) Rough primary surface textures such as those seen in volcanic flows.

(3) A thin veneer of wind-rippled sediments that overlie bedrock.

(4) Rock fragments in the 5–50 cm size range produced as part of an erosional process.

Analysis of the corrected PV reflectivity data (Ford and Pettengill, 1984) shows that most regions of apparently low reflectivity are instead characterized by the presence of wavelength-scale scatterers on the surface. This suggests that the first model can be ruled out as the predominant cause of the low uncorrected values of reflectivity measured for the tessera. Soils cannot be excluded altogether from the tessera, but less than 10% of Tellus Regio is characterized by $\rho_c < 0.08$, suggesting that any wide area is covered by no more than a few cm of loose soil.

Primary surface textures (model 2) resulting from volcanic flows (whether basaltic, silicic, or pyroclastic) are candidates for diffuse scattering elements. Fresh basalt flows may be rough at the 5–50 cm scale, and volcanism has clearly played an important role in the evolution of the surface of Venus. However, the regions where such textures are most likely to have been preserved are areas of known volcanic affinity, such as Beta Regio, Bell Regio, and other mapped volcanic provinces (Barsukov *et al.*, 1986). While areas within these regions display apparently low reflectivities in some cases (e.g. regions NW to NE of Beta), their geographic distributions do not correlate well with morphologic units mapped by the Venera orbiters. On the other hand, tessera stands out as a distinctly tectonic morphology and is clearly related in space to unusual surface properties. Mapping of tessera in Tellus Regio has revealed the presence of a number of small regions ($\sim$100 km) of volcanic plains (Bindschadler and Head, 1987). The largest of these regions are dark in PV SAR data and display relatively high values of reflectivity, indicating that they are predominantly smooth and rocky. Thus the only common volcanic structures with Tellus Regio do not display surface properties typical of the tessera. On the basis of these observations, we rule out model 2 as the predominant cause of 5–50 scale roughness of the tessera.

Similar inconsistencies also affect model 3. The postulated sediments must either be restricted to within the boundaries of the tessera or must be dispersed and lithified upon leaving the tessera at a rate equal to or greater than the supply rate. Otherwise, diffuse scattering effects would extend into the plains; this is not observed. Moreover, the corrected reflectivity data suggest that sediments have not collected in topographic lows within the tessera to depths larger than a few cm over any great areal extent. Given the uncertainty about rock-atmosphere chemical reactions under the extreme surface conditions on Venus, model 3 cannot be completely ruled out as a possible cause of diffuse scattering. However, available data suggest that it can be ruled out as the dominant cause of diffuse scattering in the tessera.

Model 4 predicts the presence of abundant rock fragments on the surface of the tessera due to an erosional process. The close association of the geologic unit boundaries of the tessera with surface properties suggests that the diffuse scattering elements present there may be linked to either the origin or present form of the tessera. Several models have been proposed and are currently under investigation to explain the unusual morphology of the tessera. These include (1) uplift and deformation due to mantle flow (Basilevsky, 1986; Sukhanov, 1986), (2) horizontal compression, possibly followed by gravitational relaxation (Bindschadler and Head, 1987), and (3) construction in a process analogous to terrestrial seafloor spreading (Bindschadler and Head, 1988c). Each of these processes involves deformation of the surface and the creation of topographic slopes. During such deformation, the surface would be disrupted. The creation of topographic slopes would lead to the downslope movement of blocks thus creating talus slopes.

The possibility that altitude-dependent chemical reactions produce small scale roughness can be suggested by the observation that α shows some correlation with elevation, as does rms slope (Pettengill *et al.*, 1980a). But although there is some correlation of α with elevation, the correlation is far from simple. For example, at an elevation of less than 2 km in the plains north of Thetis Regio ($\sim 120°$ E) values of α are as high as those found in Thetis at over 4 km. The greatest values of α within Beta Regio are associated with Devana Chasma and with a subtle (~ 0.5 km) topographic high on the eastern periphery of the domal rise (30° N, 300° E), not the topographic peak of Beta in the vicinity of Theia and Rhea Mons. Thus, although altitude-dependent reactions may contribute to this erosional process, they do not appear to dominate it.

A mass-wasting process has been proposed to explain the rock fragments in the 30 to 70 cm size range that populate the surface at the Venera 9 landing site (31.7° N, 190° E) (Florenksy *et al.*, 1977; Garvin *et al.*, 1984a). Examination of the uncorrected reflectivity data within 1° of the landing site show values of $\rho \leqslant 0.10$, leading Garvin *et al.* (1984b) to suggest that this region is characterized by either extreme cm-scale roughness or significant amounts of soil. Corrected reflectivity data for this area are in the range of 0.11–0.15, suggesting that some diffuse scattering has occurred. Given the available information, the Venera 9 landing site may be a good analog for the small-scale surface morphology of the tessera.

Conclusions

Including the corrected reflectivity data in analysis of the 1985 NSSDC Pioneer Venus data suggests that a re-interpretation of most low-reflectivity regions on Venus is necessary. The large values of α found within regions of low uncorrected reflectivity, the consequent revision of reflectivity values upward, and the pervasive nature of this correction implies that most regions of apparent low reflectivity are characterized by a large population of wavelength-scale (5–50 cm) scatterers rather than porous material. We chose to examine diffuse scattering within the tessera because of the association of diffuse scattering to this terrain type. Diffuse scatterers may take several forms: (1) primary surface texture due to volcanic flows, (2) aeolian features analogous to sand ripples, and (3) rock fragments due to mass wasting, possibly analogous to those seen at the Venera 9 landing site. All of these models are plausible, but we consider the model most consistent with available PV and Venera 15/16 data to be a mass wasting process linked to the formation of topographic slopes during the tectonic deformation that formed the tessera.

Synoptic data on the radar properties of the surface constitutes valuable information for understanding the geology of Venus, especially when examined along with high resolution data such as that obtained by Venera 15/16. For example, the correspondence of diffuse scattering to low values of uncorrected reflectivity and with tectonic deformation suggests that PV data can predict the distribution of terrain types such as the tessera. We are currently engaged in evaluating a prediction of the distribution of tessera (Kreslavsky *et al.*, 1987) using PV SAR an Arecibo data (Bindschadler *et al.*, 1988). Such a prediction can be useful for targeting areas of interest during the early stages of analysis of Magellan data.

Acknowledgements

We thank Ellen Stofan and Scott Murchie for constructive criticism. Discussions with Peter Ford on PV altimeter and SAR data were invaluable. We gratefully acknowledge the support of NASA grant NAGW-713, NASA contract JPL-957088, and the William Marlar Foundation.

References

Barsukov, V. L., Basilevsky, A. T. *et al.* (28 others): 1986, *Proc. Lunar Planet. Sci. Conf. 16th*, **91**, D378–D398.

Basilevsky, A. T.: 1986, *NASA TM-88508*, translation from *Geotektonika*, No. 4, 42–53.

Basilevsky, A. T., Pronin, A. A., Ronca, L. B., Kryuchkov, V. P., Sukhanov, A. L., and Markov, M. S.: 1986, *Proc. Lunar Planet. Sci. Conf. 16th*, **91**, D399–D411.

Bindschadler, D. L.: 1986, M.Sc. thesis, 94 pp., Brown University.

Bindschadler, D. L. and Head, J. W.: 1987, *Lunar Planet. Sci. XVIII*, 73–74.

Bindschadler, D. L. and Head, J. W.: 1988a, 'Characterization of Venera 15/16 Geologic Units from Pioneer Venus Reflectivity and Roughness Data', (in prep.)

Bindschadler, D. L. and Head, J. W.: 1988b, 'Definition and Characterization of Subtypes of the Venus Tesserae, *Lunar Planet. Sci. XIX*, 76–77.

Bindschadler, D. L. and Head, J. W.: 1988c, 'Models for the Origin of Tessera Terrain on Venus', *Lunar Planet. Sci. XIX*, 78–79.

Bindschadler, D. L., Head, J. W., Kreslavsky, M. A., Shkuratov, Yu. G., and Basilevsky, A. T.: 1988, 'Distribution of Tessera on Venus: Prediction Using Pioneer Venus and Venera Data', *Lunar Planet. Sci. XIX*, 80–81.

Campbell, D. B., Head, J. W., Harmon, J. H., and Hine, A. A.: 1984, *Science*, **226**, 167–170.
Crumpler, L. S., Head, J. W., and Campbell, D. B.: 1986, *Geology*, **14**, 1031–1034.
Florensky, C. P., Ronca, L. B., Basilevsky, A. T., Burba, G. A., Nikolaeva, O. V., Pronin, A. A., Trakhtman, A. M., Volkov, V. P., and Zazetsky, V. V.: 1977, *Geol. Soc. Am. Bull.*, **88**, 1537–1545.
Ford. P. G. and Pettengill, G. H.: 1984. *Bull. Am. Astron. Soc.*, **16**, 697.
Garvin, J. B., Head, J. W., Zuber, M. T., and Helfenstein, P.: 1984a, *J. Geophys. Res.*, **89**, 3381–3399.
Garvin, J. B., Head, J. W., and Basilevsky, A. T.: 1984b, *Lunar Planet, Sci. XV*, 292–293.
Garvin, J. B., Head, J. W., Pettengill, G. H. and Zisk, S. H.: 1985, *J. Geophys. Res.*, **90**, 6859–6871.
Hagfors, T.: 1964, *J. Geophys. Res.*, **69**, 3775–3784.
Hagfors, T.: 1967, *Radio Sci.*, **2**, 445–465.
Hagfors, T.: 1970, *Radio Sci.*, **5**, 189–227.
Head, J. W., and L. S. Crumpler: 1987, *Science*, **238**, 1380–1385.
Head, J. W., Peterfreund, A. R., Garvin, J. B., and Zisk, S. H.: 1985, *J. Geophys. Res.*, **90**, 6873–6885.
Kotelnikov, V. A., Bogomolov, A. F. and Rzhiga, O. N.: 1985, *Adv, Space Res.*, **5**, 5–16.
Kreslavsky, M. A., Basilevsky, A. T., and Shkuratov, Yu. G.: 1988, *Astron. Vestn.* (in press) (in Russian).
Krotikov, V. D. and Troitsky, V. S.: 1963, *Usp. Fiz. Nauk.*, **5**, 1057–1061 (in Russian).
Masursky, H., Eliason, E., Ford, P. G., McGill, G. E., Pettengill, G. H., Schaber, G. G., and Schubert, G.: 1980, *J. Geophys, Res.*, **85**, 8232–8260.
Olhoeft, G. R. and Strangway, D. W.: 1975, *Earth Planet. Sci. Lett.*, **24**, 394–404.
Pettengill, G. H., Eliason, E., Ford, P. G., Loriot, G. B., Masursky, H., and McGill, G. E.: 1980a, *J. Geophys. Res.*, **85**, 8261–8270.
Pettengill, G. H., Harwood, D. F., and Keller, G. H.: 1980b, *IEEE Trans. Geosci. Rem. Sens.*, **GE-18**, 28–32.
Pettengill, G. H., Ford, P. G., and Nozette, S.: 1982, *Science*, **217**, 640–642.
Schaber, G. G.: 1982, *Geophys. Res. Lett.*, **9**, 499–502.
Sharpton, V. I., and Head, J. W.: 1985, *J. Geophys. Res.*, **90**, 3733–3740.
Simpson, R. A., Tyler, G. L., and Schaber, G. G.: 1984, *J. Geophys. Res.*, **89**, 10,385–10,404.
Sukhanov, A. L.: *Geotektonika*, No. 4, 60–76 (in Russian).
Tyler, G. L. and Howard, H. T.: 1973, *J. Geophys. Res.*, **76**, 4852–4874.
Tyler, G. L., Campbell, D. B., Downs, G. S., Green, R., and Moore, H. J.: 1976, *Science*, **193**, 812–815.
U.S.G.S.: 1981, *Altimetric and Shaded Relief Map of Venus*, Map I-1324.